Addition of V_2O_5 and V_2O_3 to the GTOX Oxide database

GTT-Technologies, Herzogenrath

GTT-Workshop, 27-29. June 2018, Herzogenrath

Klaus Hack, Tatjana Jantzen

Addition of VO_x

Vanadium

V as alloying element in steel products for improving their tensile strength, fatigue performance and heat resistance.

In chemical industries, V compounds are utilized as a desulfurization catalyst in sulfuric acid production processes.

Vanadium-Titanium alloys as new electrode materials in hydrogen storage batteries.

The desulfurization is important in the iron and steel industry.

Contents of presentation

GTT-Technologies

- Introduction
- Binary systems
  - V-O [Yang15]
- Quasi-binary systems
  - Al_2O_3-V_2O_5
  - CaO-V_2O_5
  - Cr_2O_3-V_2O_5
  - FeO-V_2O_3, Fe_2O_3-V_2O_5
  - MgO-V_2O_5 , MgO-V_2O_3
  - MnO-V_2O_5, Mn_2O_3-V_2O_5
  - NiO-V_2O_5
  - TiO_x-V_2O_3 [Yang17]
  - SiO_2-V_2O_3, SiO_2-V_2O_5
- Ternary systems
  - Al_2O_3-Fe_2O_3-V_2O_5
  - Al_2O_3-FeO-V_2O_3
  - Al_2O_3-V_2O_5-SiO_2
  - CaO-Fe_2O_3-V_2O_5
  - CaO-NiO-V_2O_5
  - CaO-SiO_2-V_2O_5
  - TiO_2-Ti_2O_3-V_2O_3

Introduction

The associate species were added in order to describe the liquid phase in VO_x-containing systems. The composition of the liquid oxide species are as introduced by Spear taking two moles of cations per associate. Species for similar systems are modelled in the same way, i.e. using the same stoichiometry.

System	Associate species	Used data for Gibbs energy
V-O	*V, $V_2O_2^*$, V_2O_3, V_2O_4, V_2O_5*	*SGPS database*
FeO-V_2O_3	*FeV_2O_4*	*This work*
MgO-V_2O_3	*MgV_2O_4*	*This work*
MnO-V_2O_3	*MnV_2O_4*	*This work*

** H_f changed in this work.*

Modelling of V-containing phases

Phase	Description
fcc-A1	(Al, Ca, Fe, Cr, P, Mg, Mn, S, Si, Zn, Ti, O, **V**) (Va)
bcc-A2	(Al, Ca, Fe, Cr, P, Mn, S, Zn, Ti, O, TiO_3, **V**, **VO_3**)$(Va)_3$
cub-A13	(Cr, Fe, Mg, Mn, **V**)
cbcc-A12	(Cr, Fe, Mg, Mn, **V**)
Titania Spinel	$(Fe^{+2},Fe^{+3},Mg^{+2},Mn^{+2},Ti^{+4})(Al^{+3},Fe^{+2},Fe^{+3},Mg^{+2},Mn^{+2},Mn^{+3},Va,Ti^{+3},\mathbf{V^{+3}})_2\,(O^{-2})_4$
PSbrookite-Ti_3O_5	$(Al, Mg, Fe, Mn, Ti, \mathbf{V})_1(Al,Ti, Fe)_1(Ti)_1(O)_5$
$MeVO_4$	$(Al^{+3}, Fe^{+3})_1(\mathbf{V^{+5}})_1(O^{-2})_4$
Rutile	$(Ti, \mathbf{V})_1(\underline{O,}\ Va)_2$
Sigma	$(\underline{Fe, Mn})_8(Cr, \mathbf{V})_4(Cr, Fe, Mn, \mathbf{V})_{18}$
Beta	(**V**) (O,Va)
C2S-C3P	$(\underline{Ca^{+2}},Cr^{+2},Mg^{+2},Mn^{+2})_3(\underline{Ca^{+2}},\underline{Va})(\underline{P^{+5}},\underline{Si^{+4}},\mathbf{V^{+5}})_2(O^{-2})_8$
Gamma	$(\mathbf{V})\ (O,\underline{Va})_{0.5}$
Corundum	$(\underline{Al^{+3}},Cr^{+2},\underline{Cr^{+3}},\underline{Fe^{+3}},\underline{Mn^{+3}},\ \underline{Ti^{+3}},\underline{Fe_{0.5}Ti_{0.5}}^{+3},\underline{Mg_{0.5}Ti_{0.5}}^{+3},\ \underline{Mn_{0.5}Ti_{0.5}}^{+3},\ \underline{\mathbf{V^{+3}},}\ \mathbf{V^{+4}})_2$ $(Cr^{+3},Va)_1(O^{-2})_3$
V_3O_5 and M_8O_{15}	$(\mathbf{V}, Ti)_3(O)_5$ and $(\underline{\mathbf{V},}\ \underline{Ti})_8(O)_{15}$
T_5O_9 and V_5O_9	$(\mathbf{V}, \underline{Ti})_3(O)_5$ and $(\underline{\mathbf{V},}\ Ti)_3(O)_5$
M_4O_7 and M_6O_{11}	$(\underline{\mathbf{V},}\ \underline{Ti})_4(O)_7$ and $(\underline{\mathbf{V},}\ \underline{Ti})_6(O)_{11}$
MeO	$(Al^{+3},Ca^{+2},Cr^{+3},Fe^{+2},Fe^{+3},Mg^{+2},Mn^{+2},Mn^{+3},Ti^{+4},Ti^{+3},\mathbf{V^{+2}},\mathbf{V^{+3}},\mathbf{V},\ Zn^{+2},Va)(O^{-2})$

Modelling of the phases in ternary systems

System	*Phase*	*Description*	*Used data*
Al_2O_3-FeO-V_2O_3	Titania Spinel	$(Fe^{+2},Fe^{+3})(Al^{+3},Fe^{+2},Fe^{+3},V^{+3},Va)_2\ (O^{-2})_4$	Present work
Al_2O_3-Fe_2O_3-V_2O_5	$MeVO_4$	$(\underline{Al^{+3}},\underline{Fe^{+3}})_1(V^{+5})_1(O^{-2})_4$	Present work
CaO-Fe_2O_3-V_2O_5	$Ca_6Fe_7V_3O_{24}$	stoichiometric	Present work
CaO-NiO-V_2O_5	$Ca_5Ni_4V_8O_{24}$	stoichiometric	Present work
CaO-SiO_2-V_2O_5	α-Ca_2SiO_4	$(Ca^{+2})_3(\underline{Ca^{+2}},Va)(V^{+5},\underline{Si^{+4}})_2(O^{-2})_8$	Present work
TiO_2-Ti_2O_3-V_2O_3	Pseudobrookite	$(Ti, V)_1(Ti)_1(Ti)_1(O)_5$	Present work
	Rutile	$(Ti, V)\ (O, Va)_2$	[Yang17]
	Ti_2VO_5	stoichiometric	[Yang17]
	T_5O_9	$(\underline{Ti},V)_5O_9$	[Yang17]
	V_3O_5	$(Ti, \underline{V})_3(O)_5$	[Yang17]
	M_4O_7	$(Ti, V)_4(O)_7$	[Yang17]
	V_5O_9	$(Ti, \underline{V})_5(O)_9$	[Yang17]
	M_6O_{11}	$(Ti, V)_6(O)_{11}$	[Yang17]
	M_8O_{15}	$(Ti, V)_8(O)_{15}$	[Yang17]

V-O phase diagram

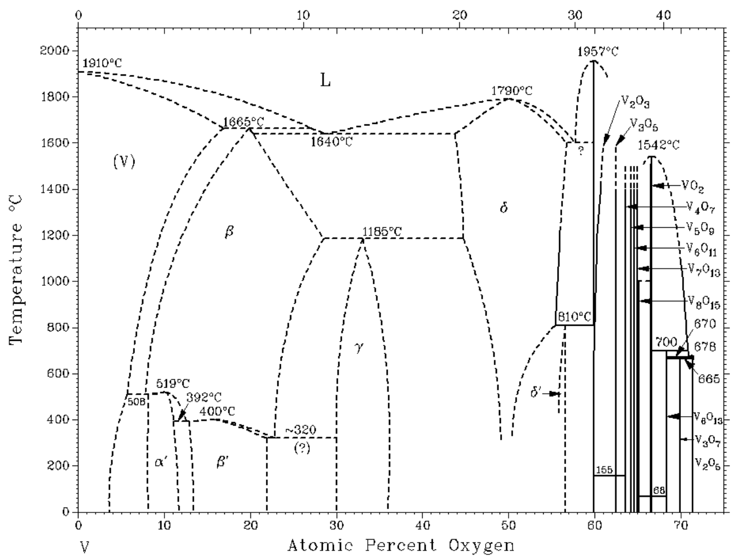

T.B. Massalski (ed), Binary Alloy Phase Diagrams, Second Edition, ASM International, Metals Park, OH 1990.

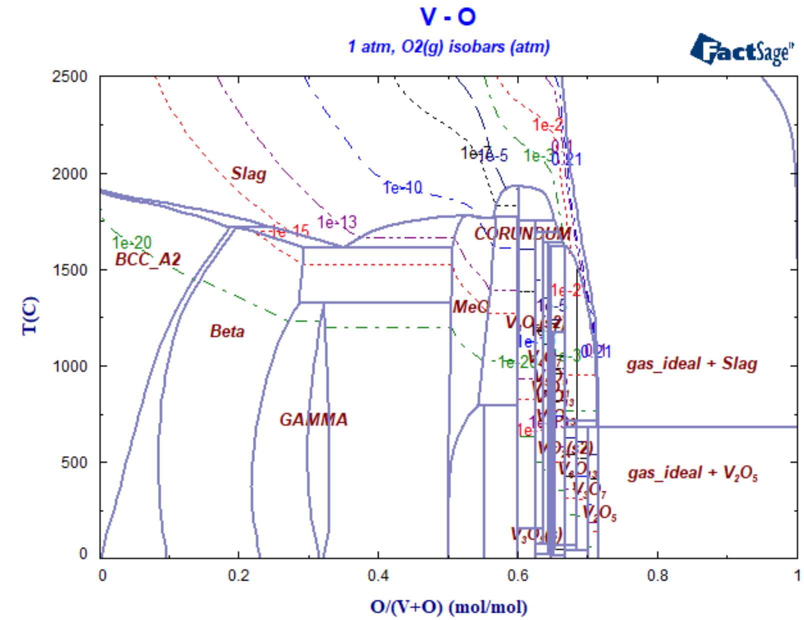

Phase	Description	Used data
Slag	(V, V_2O_2, V_2O_3, V_2O_4, V_2O_5)	Present work
Bcc-A2	(V, O, VO_3)$(Va)_3$	Present work
Beta	(V)(O, Va)	[Yang15]
Gamma	(V)$(O, Va)_{0.5}$	[Yang15]
MeO	$(V^{+2},V^{+3},V)(O^{-2})$	Present work
Corundum	$(V^{+4},V^{+3},Va)_2(O^{-2})_3$	Present work
VO, VO_2, V_2O_3,	stoichiometric	[Yang15]
V_2O_5, V_3O_5, V_3O_7,	stoichiometric	[Yang15]
V_4O_7, V_5O_9, V_6O_{11},	stoichiometric	[Yang15]
V_6O_{13},V_7O_{13},V_8O_{15},	stoichiometric	[Yang15]
$V_{52}O_{64}$	stoichiometric	[Yang15]

Al_2O_3-V_2O_5 phase diagram

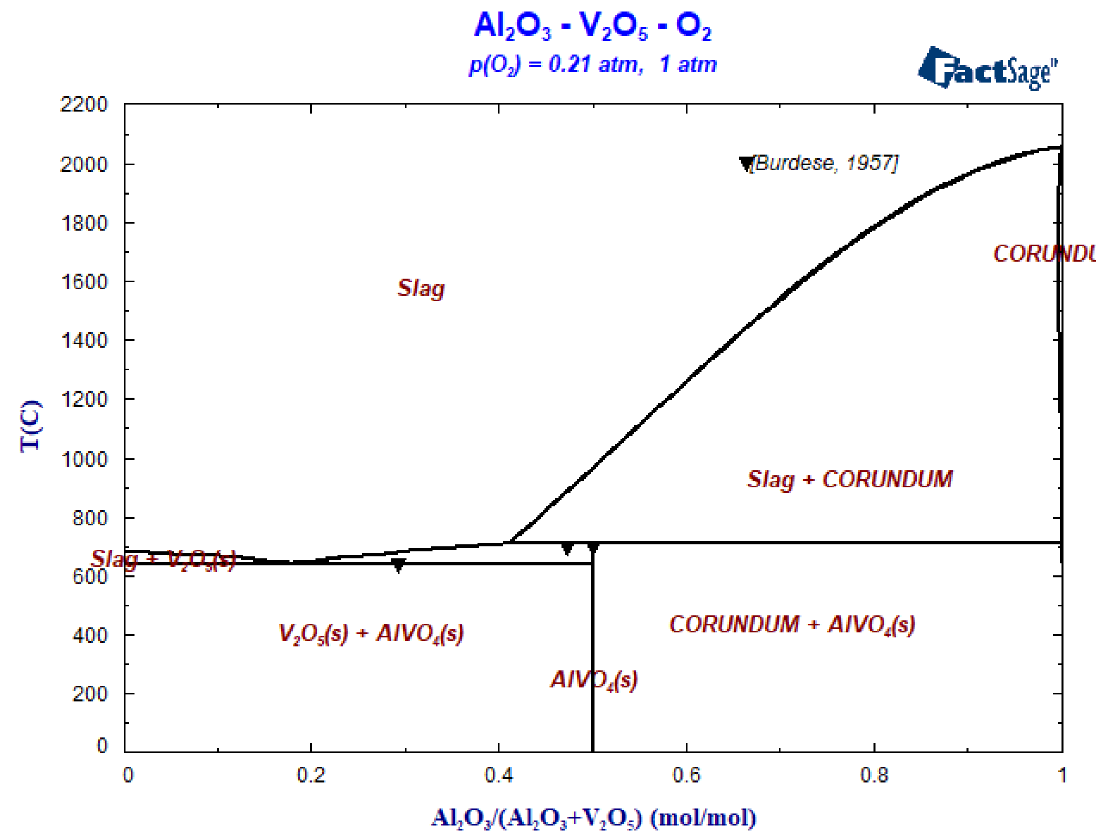

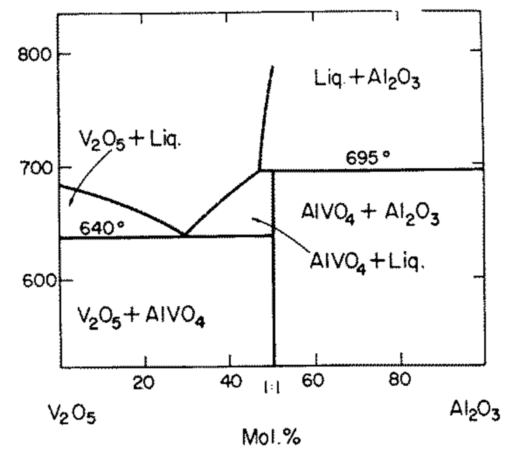

A. Burdese, Ann. Chim. (Rome), 47 [7-8], (1957), pp. 797-805.

Al_2O_3-V_2O_3 phase diagram

GTT-Technologies

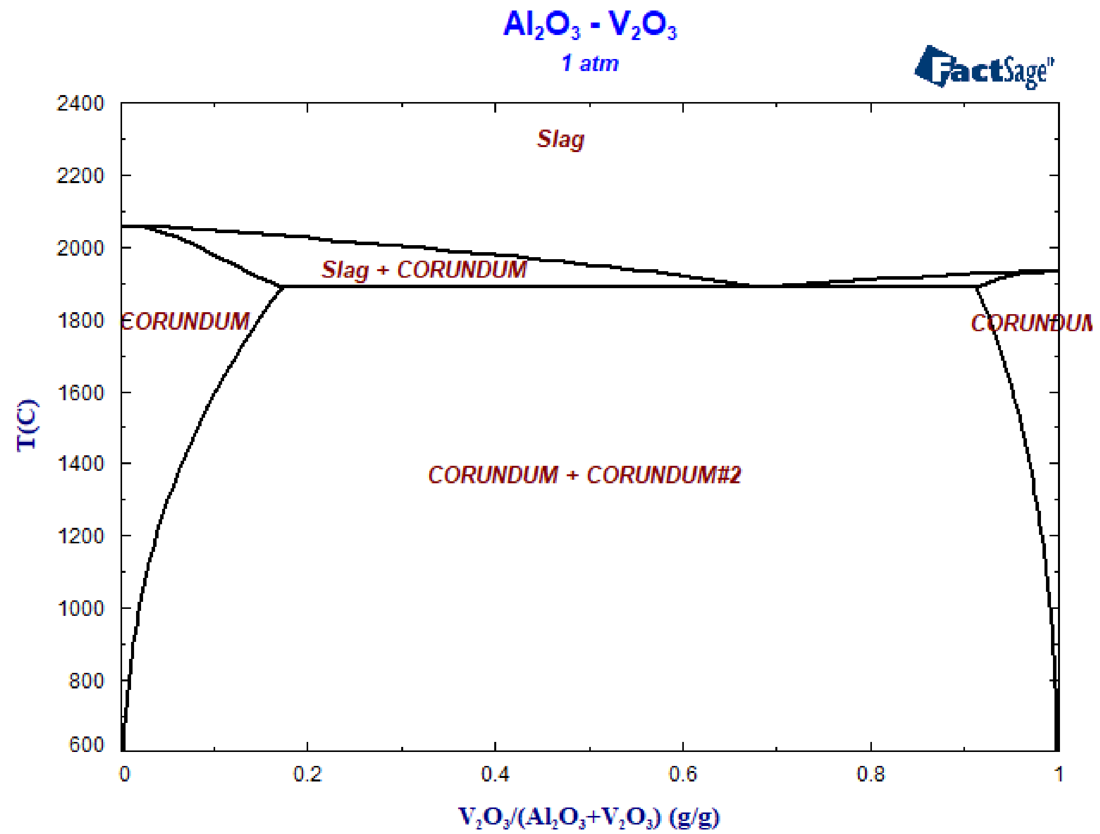

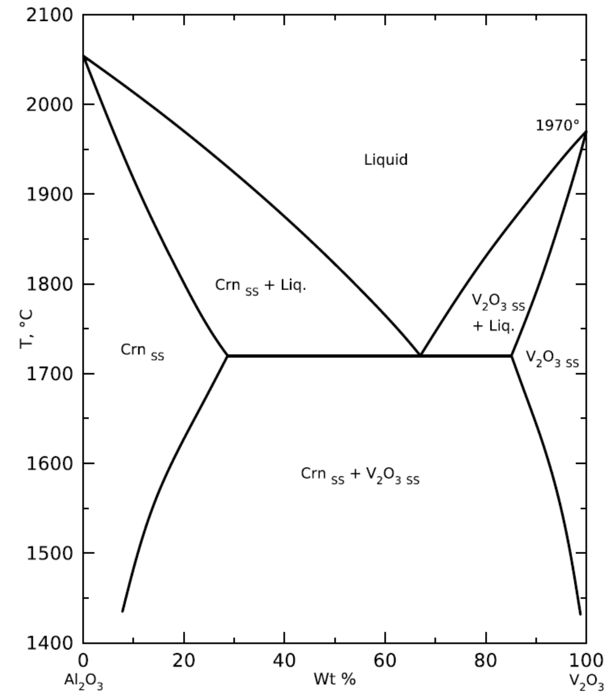

A. Muan and M. S. Najjar, "Compositions involving V2O3-Al2O3-CaO", US Patent 5,070,065, December 3, 1991.

CaO-V_2O_5 phase diagram

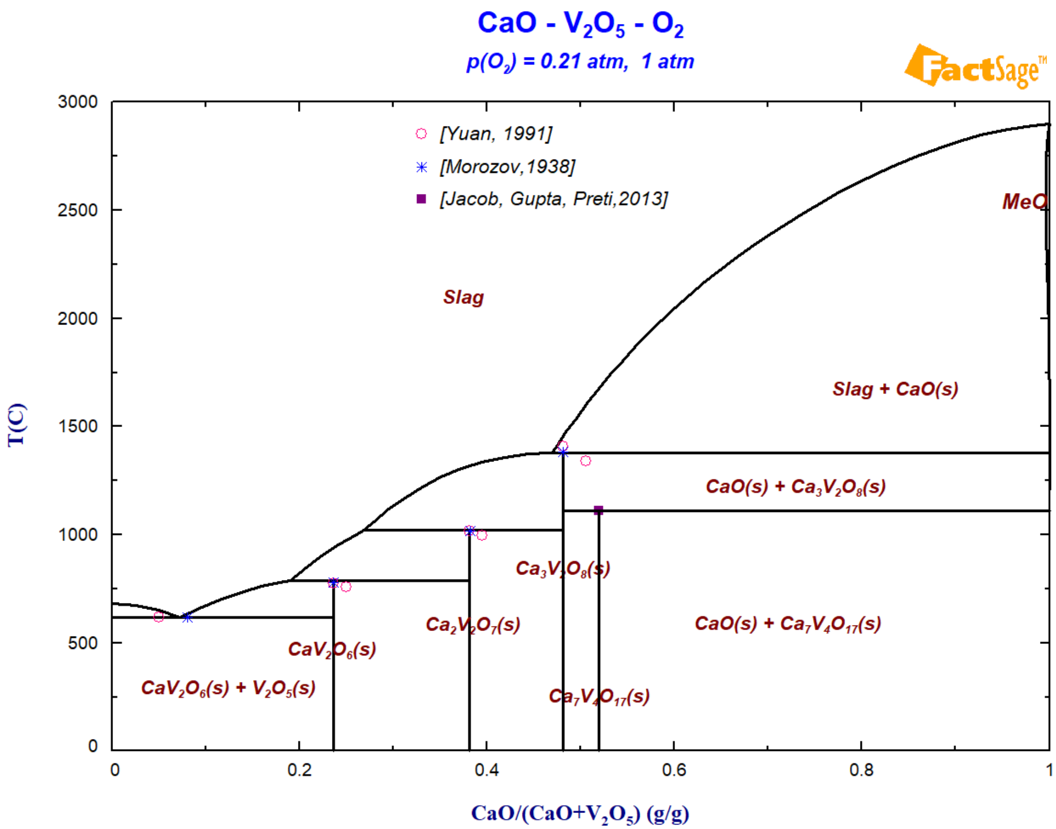

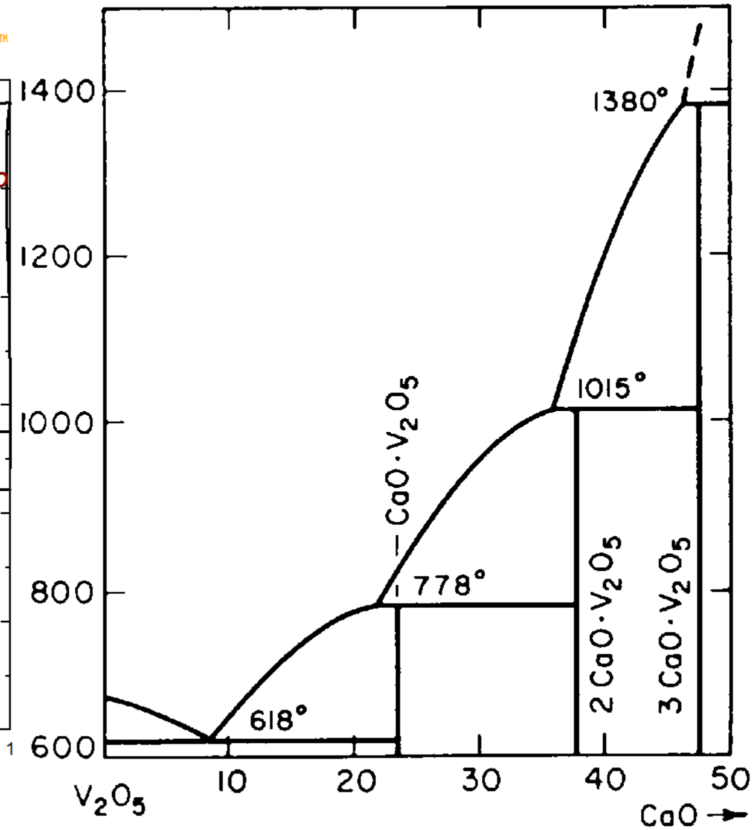

V.L.Volkov, A.A. Fotiev, L.L. Surat, Zh. Fiz. Khim., 49 [6], (1975), pp.1575-1577.

Cr_2O_3-V_2O_5 phase diagram in air

GTT-Technologies

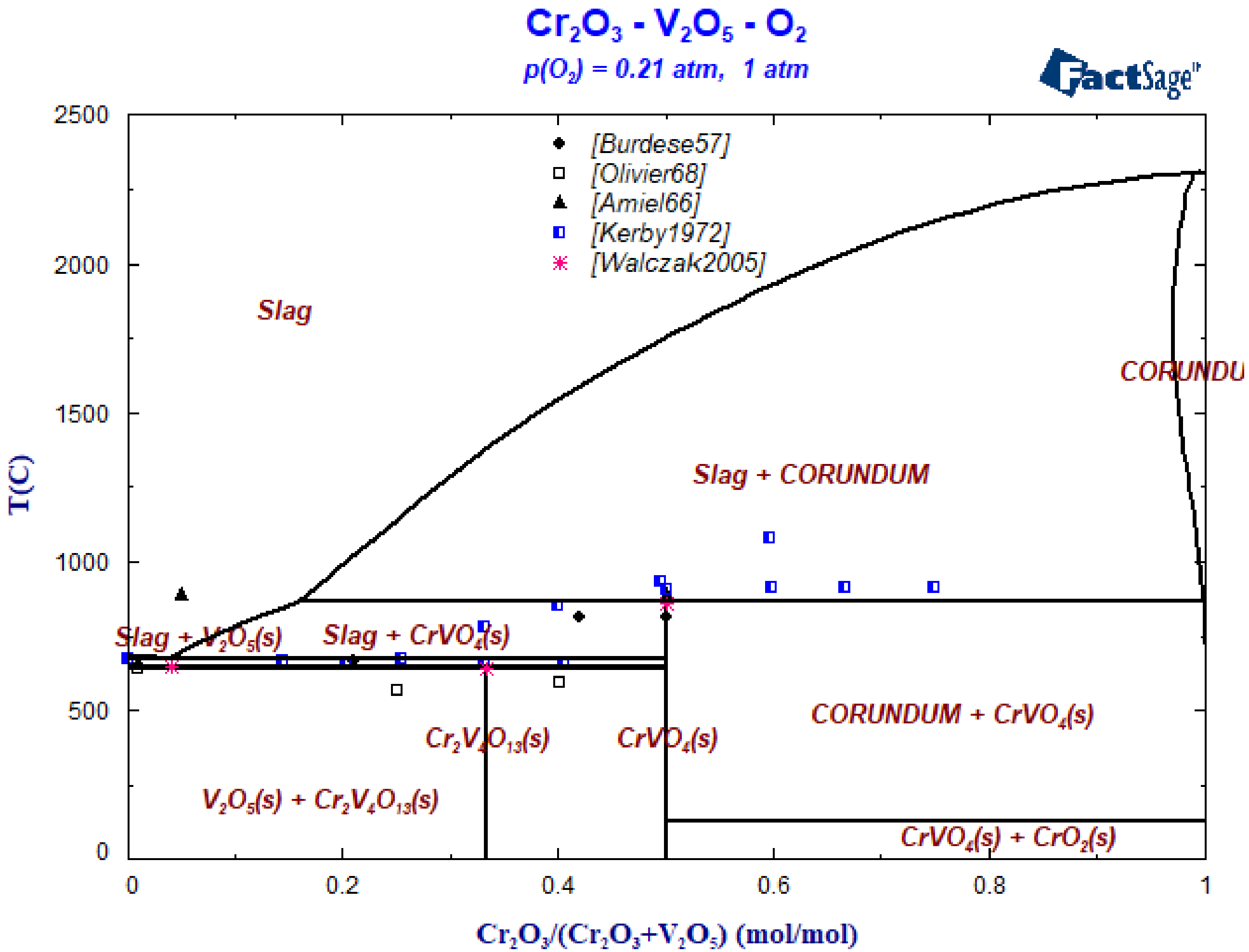

Modelling of Titania Spinel

Titania Spinel

V^{+3}

(Fe^{+2},Fe^{+3},Mg^{+2}, Mn^{+2}, Ti^{+4})

(Al^{+3},Fe^{+2},Fe^{+3},Mg^{+2}, Mn^{+2},Mn^{+3},Ti^{+3},V^{+3},Va)$_2$ (O^{-2})$_4$

Spinels with Ti_2O_3
$MgTi_2O_4$, $MnTi_2O_4$

Spinels with V_2O_3
MgV_2O_4, MnV_2O_4, FeV_2O_4

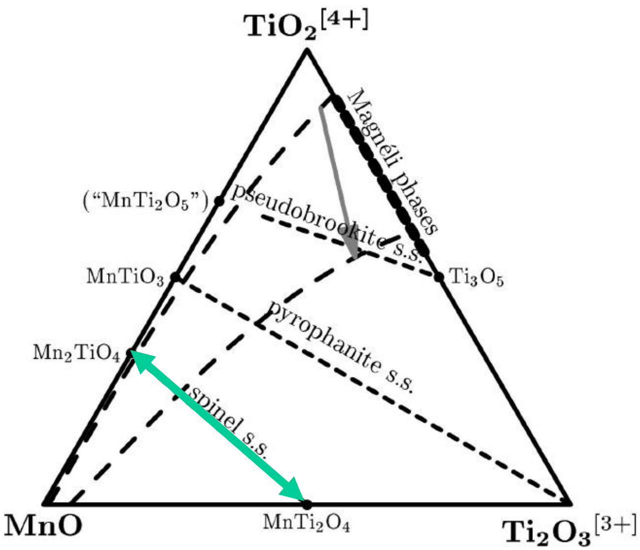

J.-B. Kang, H.-B. Lee, ISIJ Intern., 45 (2005), pp. 1543-1551.

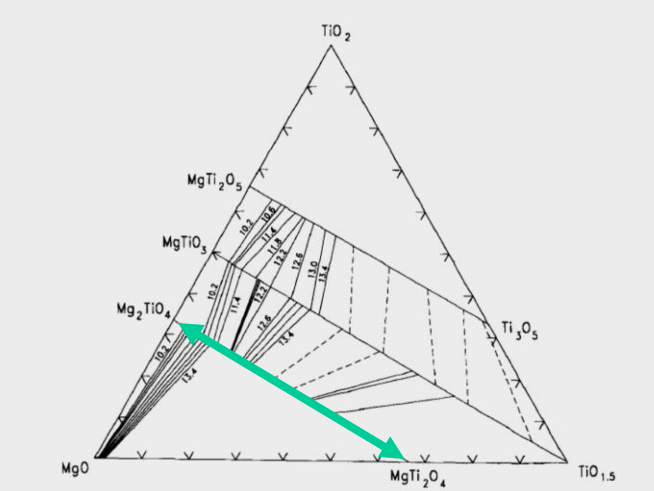

Fig. 1. Equilibrium tie-lines in the MgO-TiO_2-$TiO_{1.5}$ system at 1500°C. (Compositions in mole%). Solid lines experimental. Dashed lines calculated. Numbers written on the tie-lines are [$-\log f_{O_2}$ (bar)].

A.D. Pelton, G. Eriksson, D. Krajewski, M.Göbbels, E. Woermann, Z. Phys. Chem., 207 (1998), pp. 163-180.

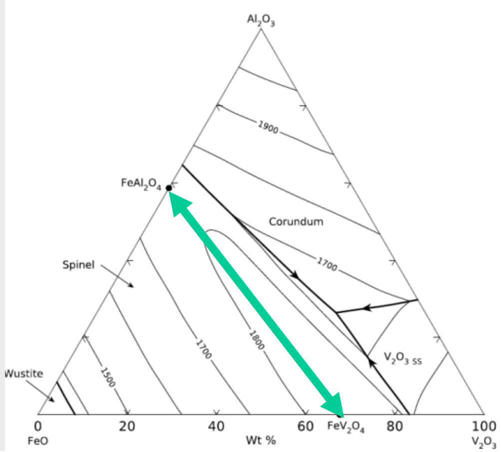

B. Leusmann, N. Jb. Miner. Mh., 12 (1979), pp. 556-559.

$FeO\text{-}V_2O_3$ phase diagram in equilibrium with Fe

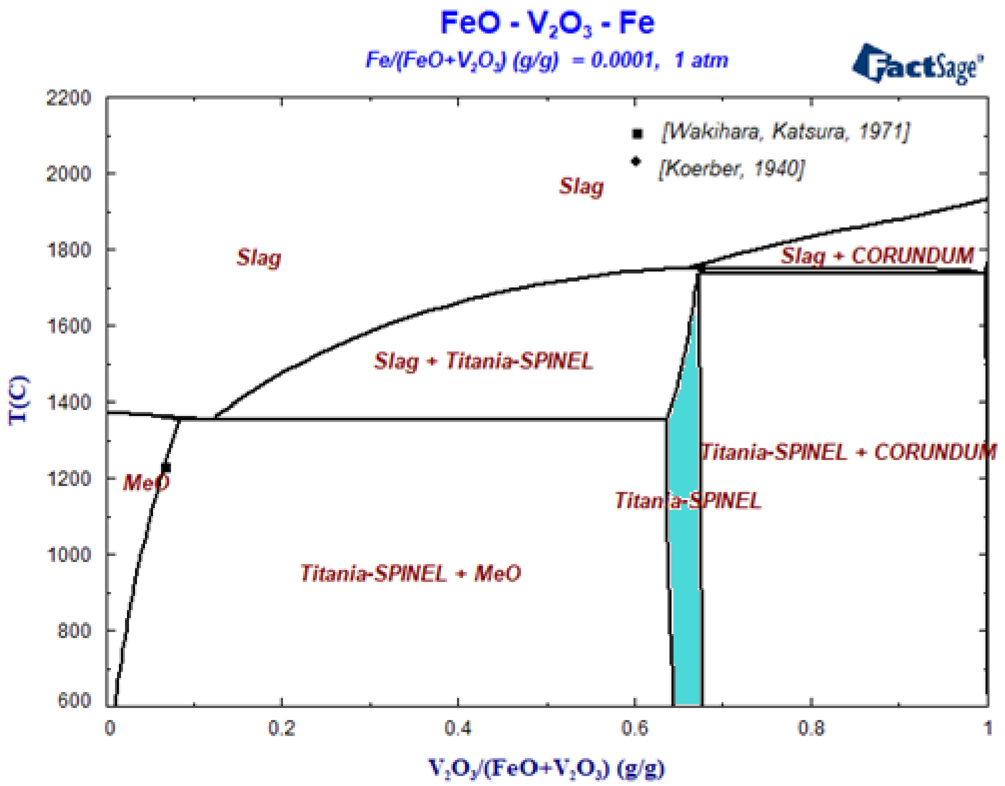

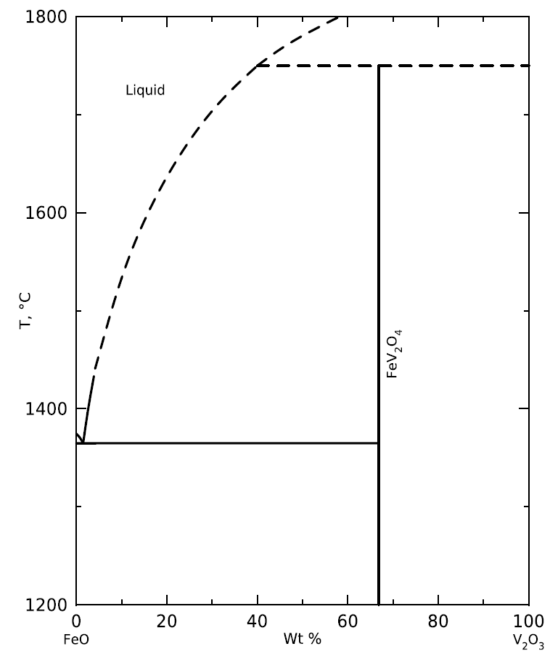

F. Koerber and W. Oelsen, Stahl Eisen, 60 [43] 948-955 (1940).

Isothermal section at 600°C in Al_2O_3-FeO-V_2O_3

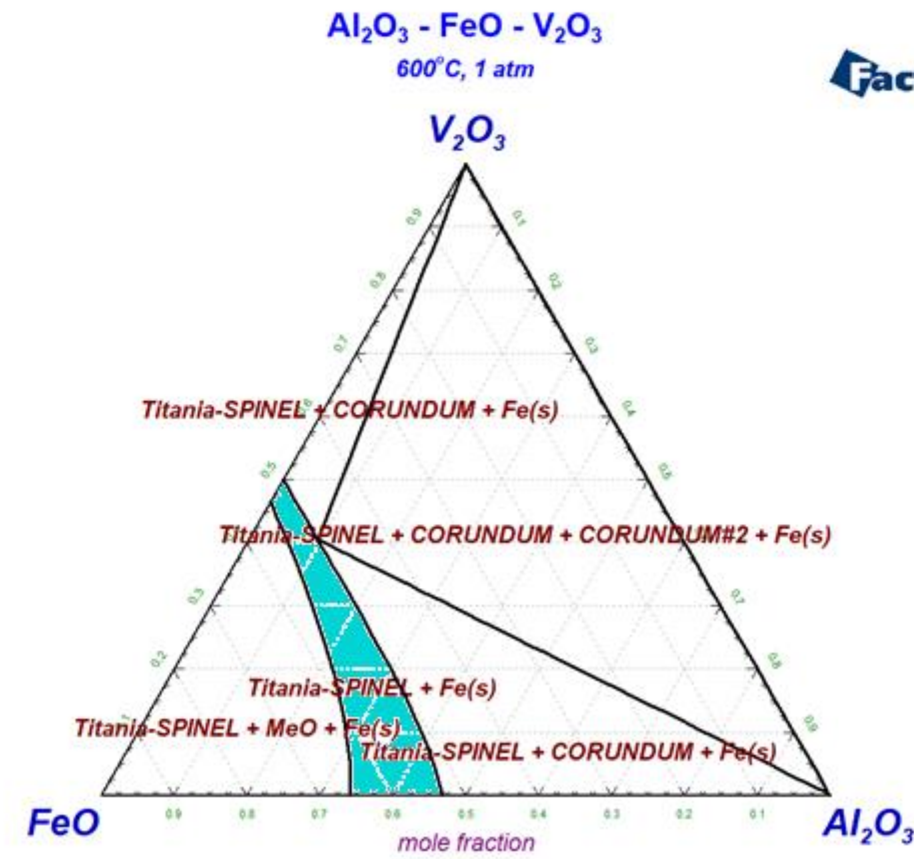

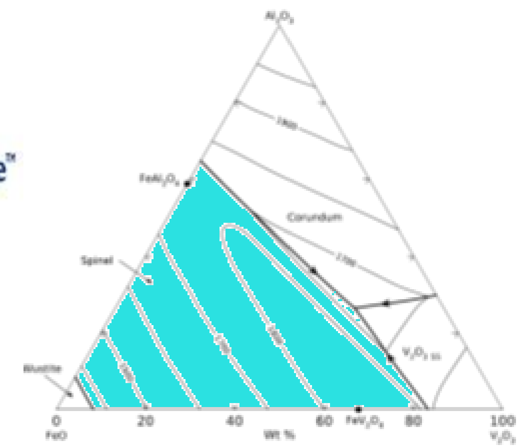

B. Leusmann, N. Jb. Miner. Mh., 12 (1979), pp. 556-559.

Fe_2O_3-V_2O_5 phase diagram in air

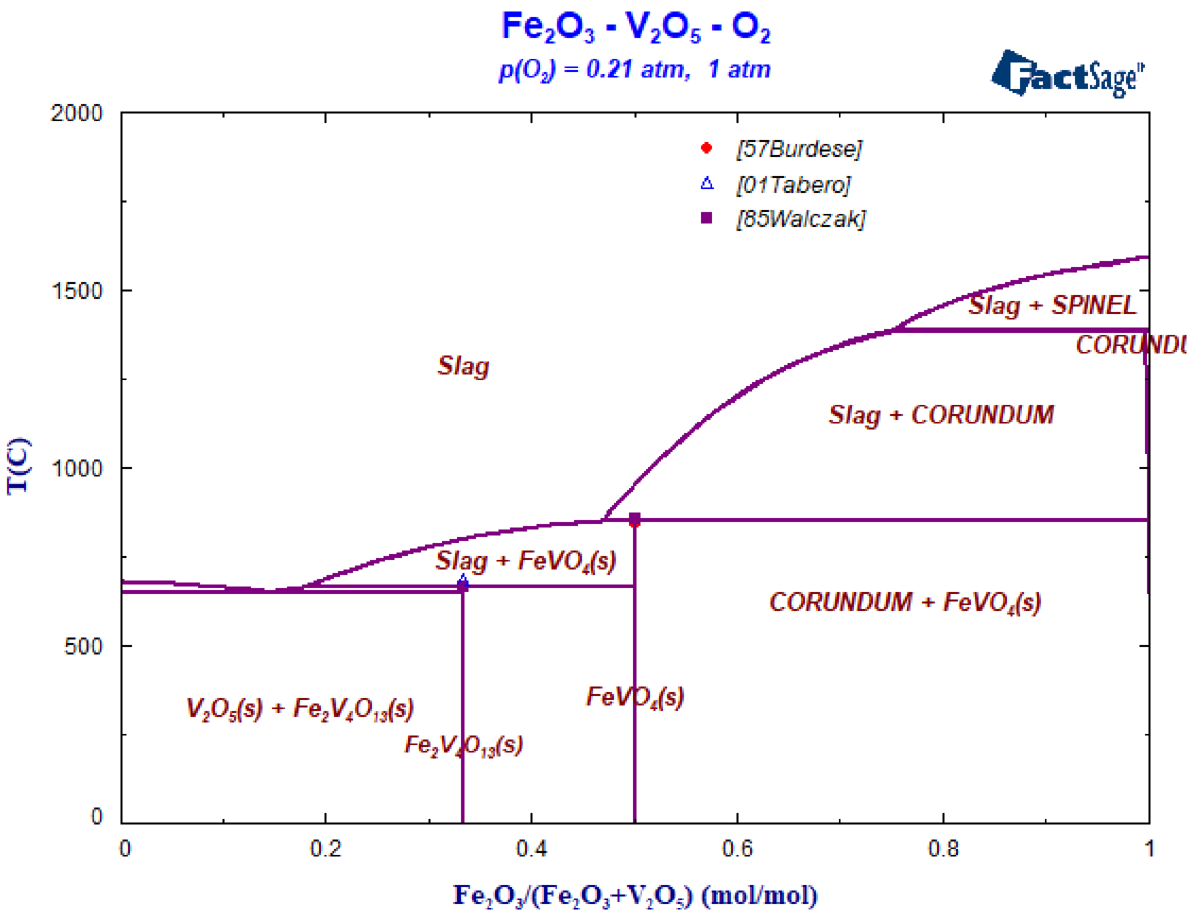

$MgO\text{-}V_2O_5$ phase diagram in air

GTT-Technologies

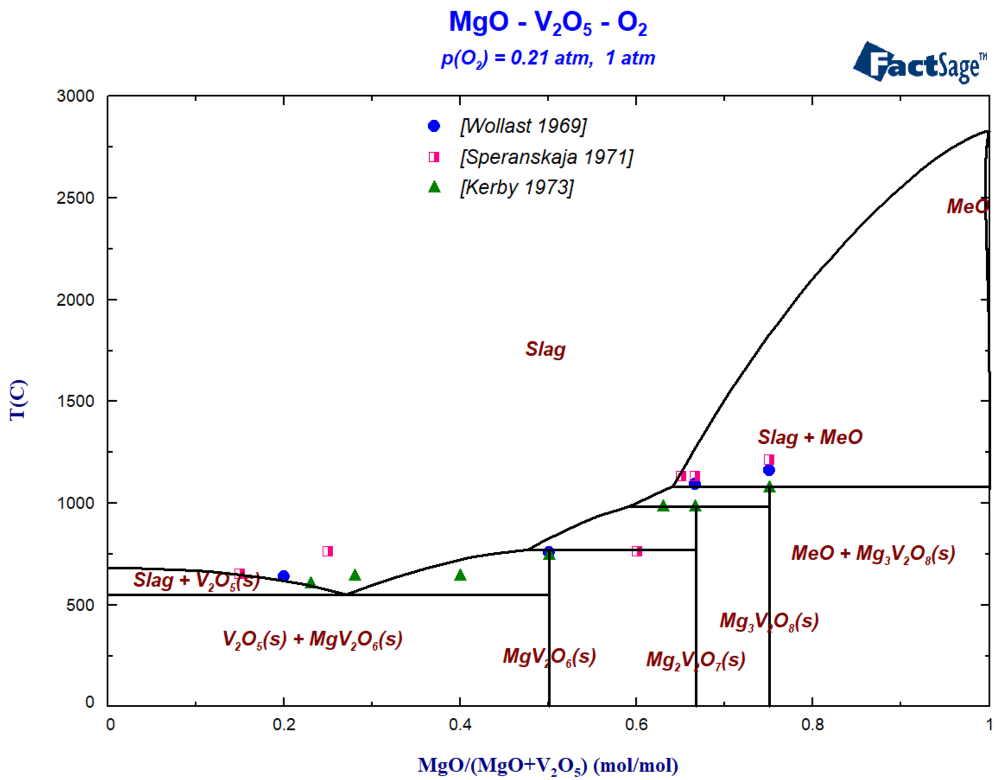

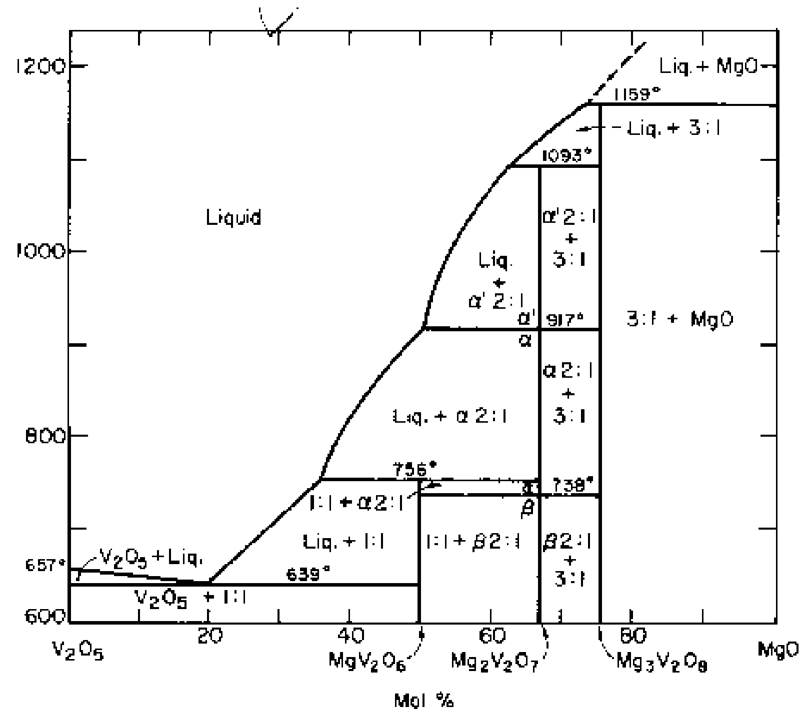

R. Wollast and A. Tazairt, Silic. Ind., 34 [2] 37-45 (1969).

MgO-V_2O_3 phase diagram

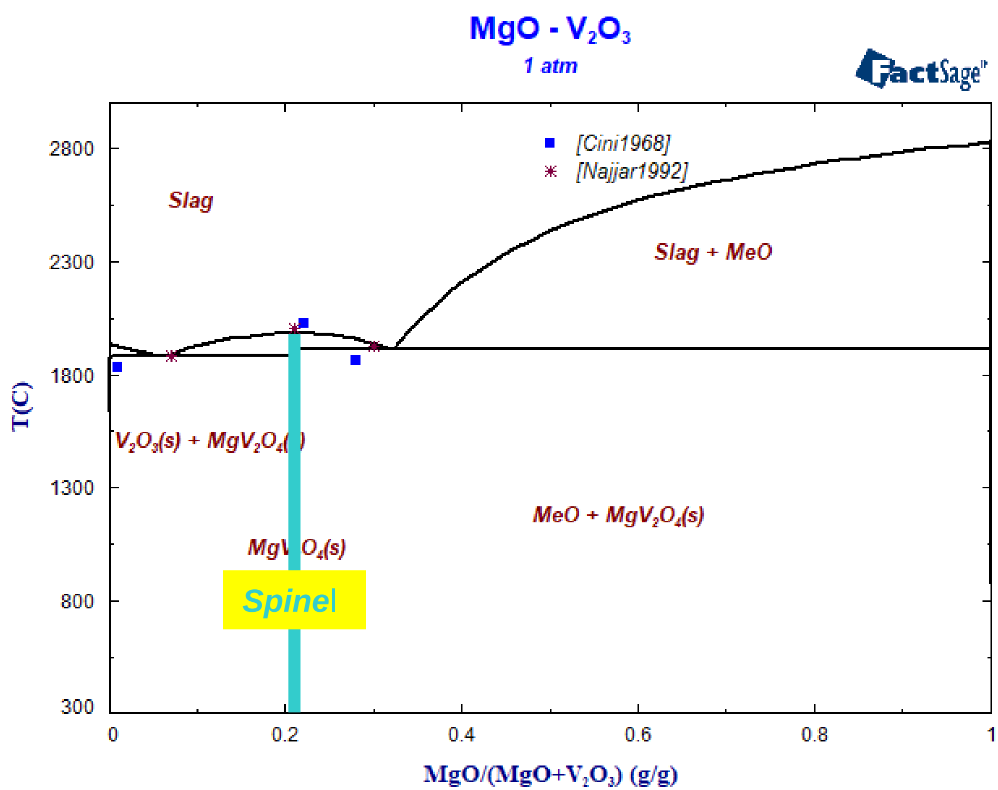

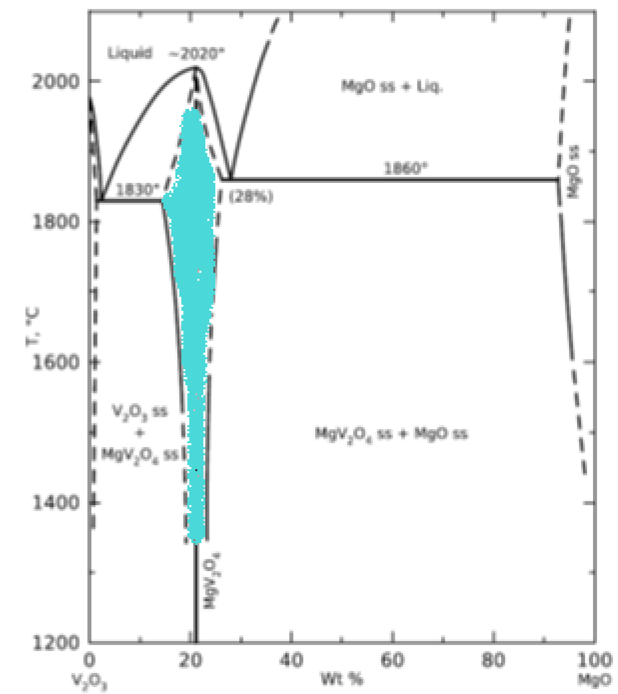

L. Cini, Radex Rundsch., No. 2, 102-112 (1968).

MnO-V_2O_5 phase diagram in equilibrium with Mn

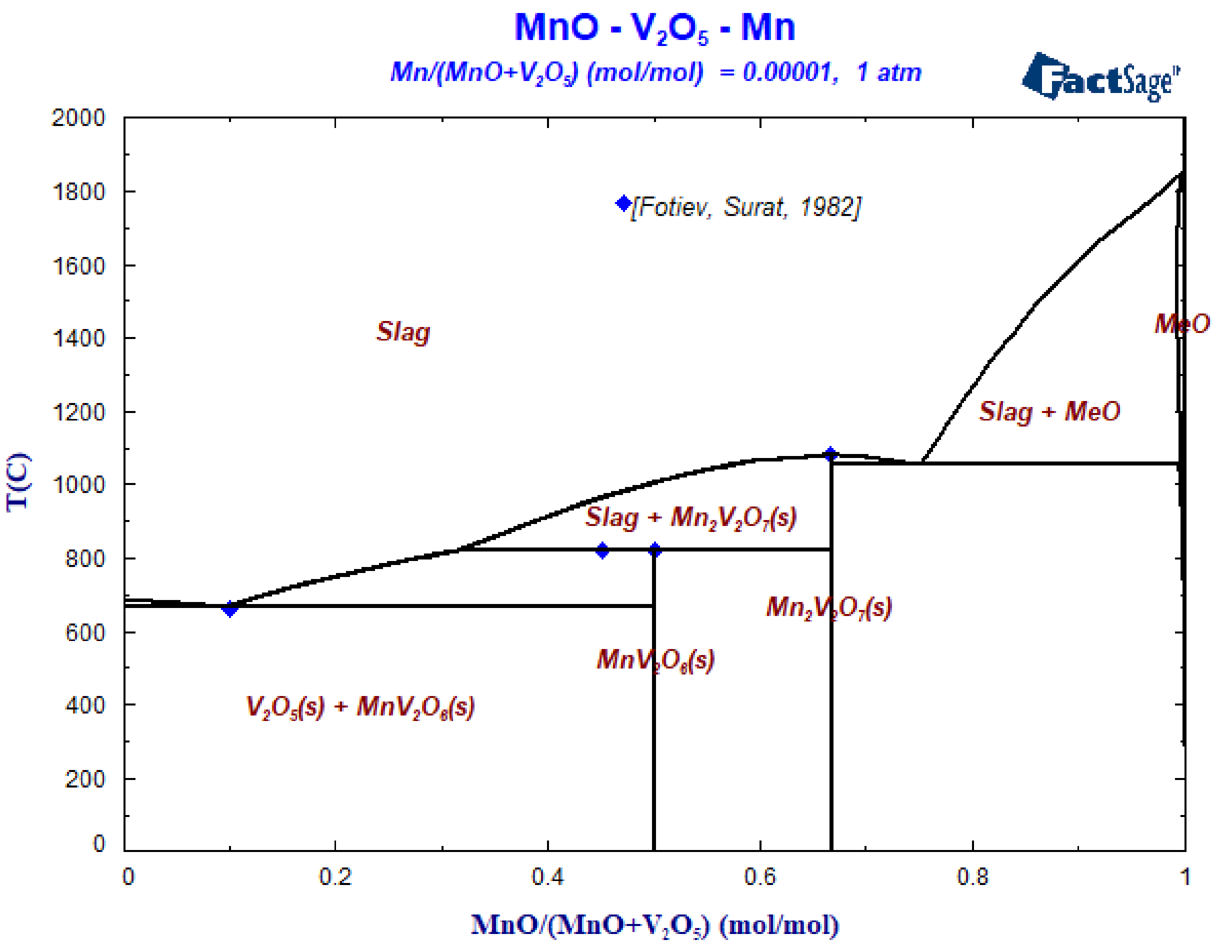

MnO-V_2O_5 phase diagram, CO/CO_2=1

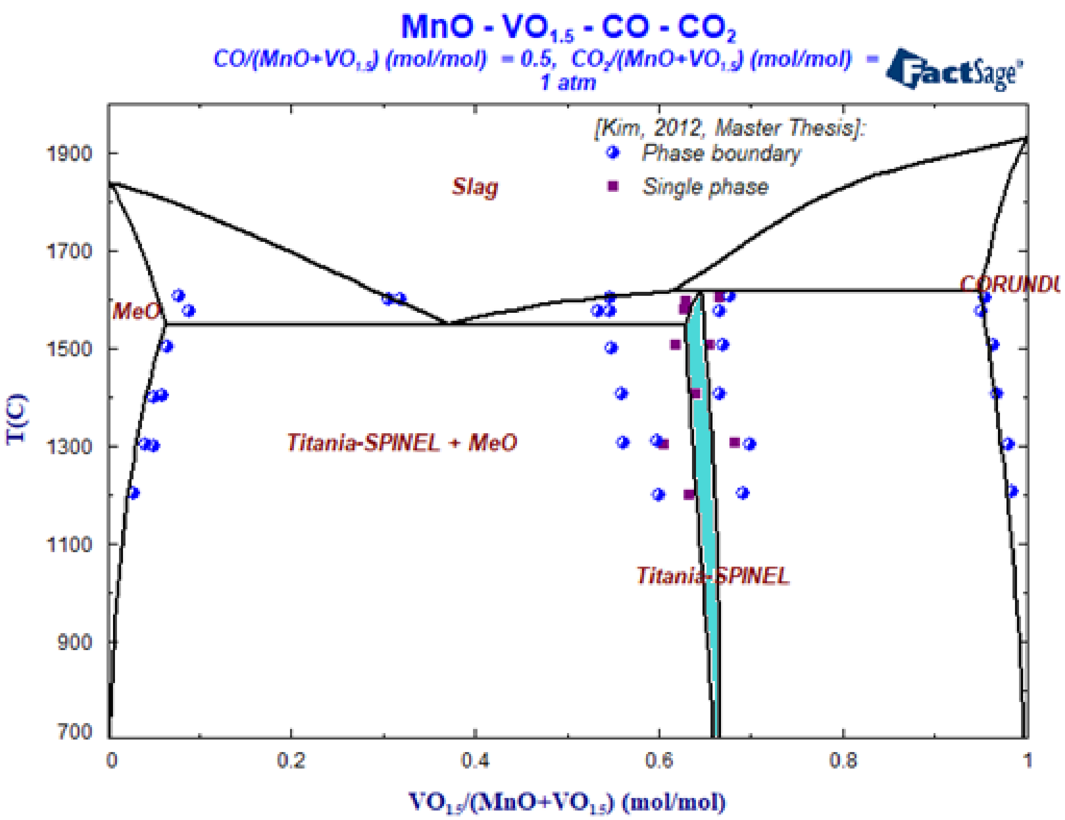

NiO-V_2O_5 phase diagram

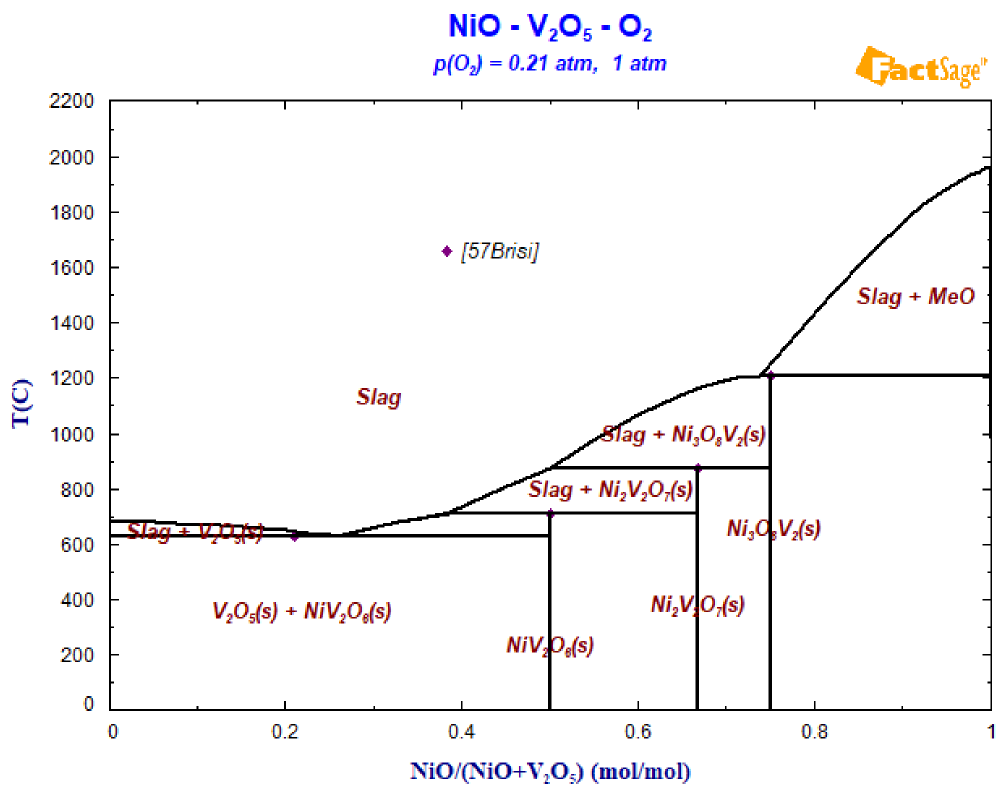

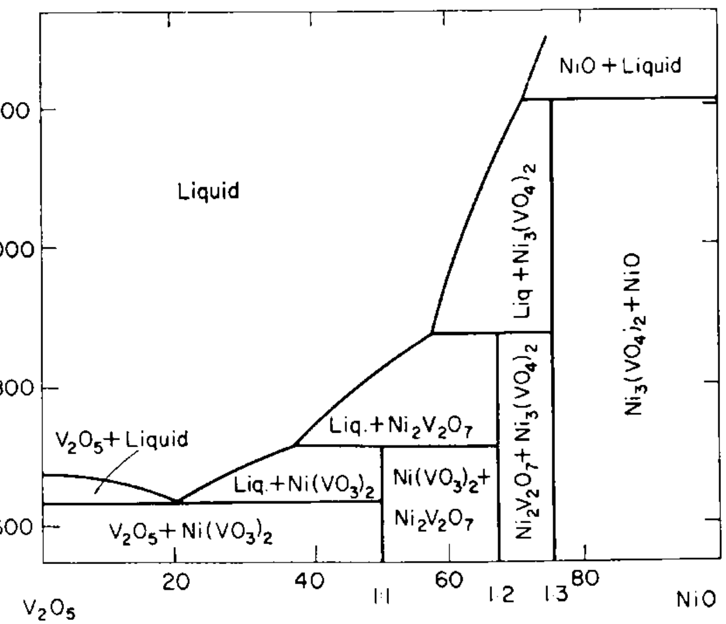

C. Brisi, Ann. Chim. (Rome), 47 [7-8], (1957), pp. 806-816.

Isothermal section at 600ºC in Al_2O_3-V_2O_5-SiO_2

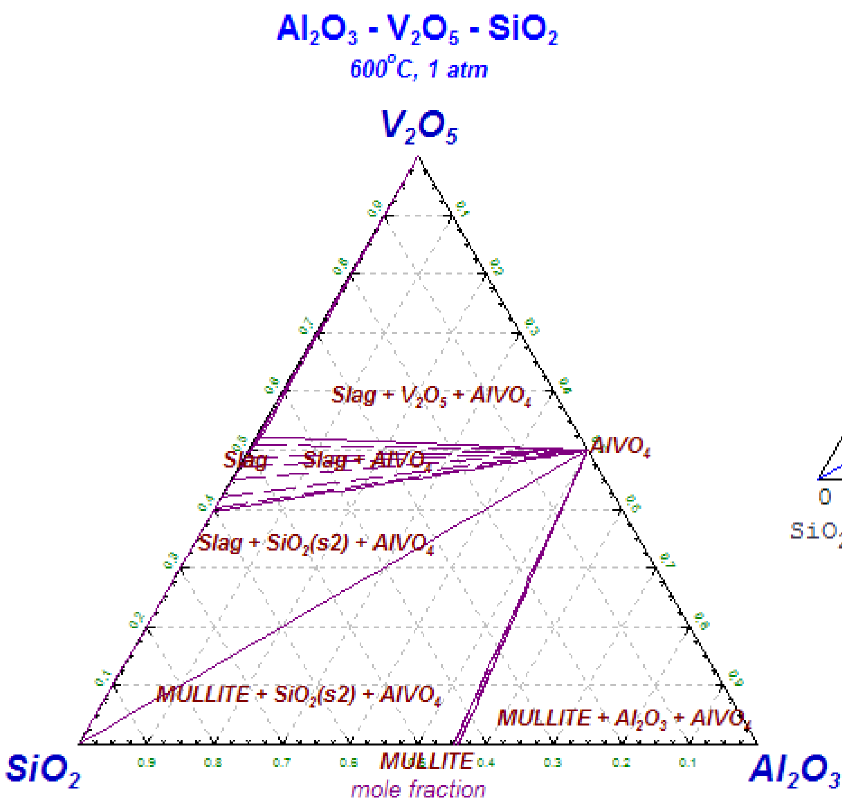

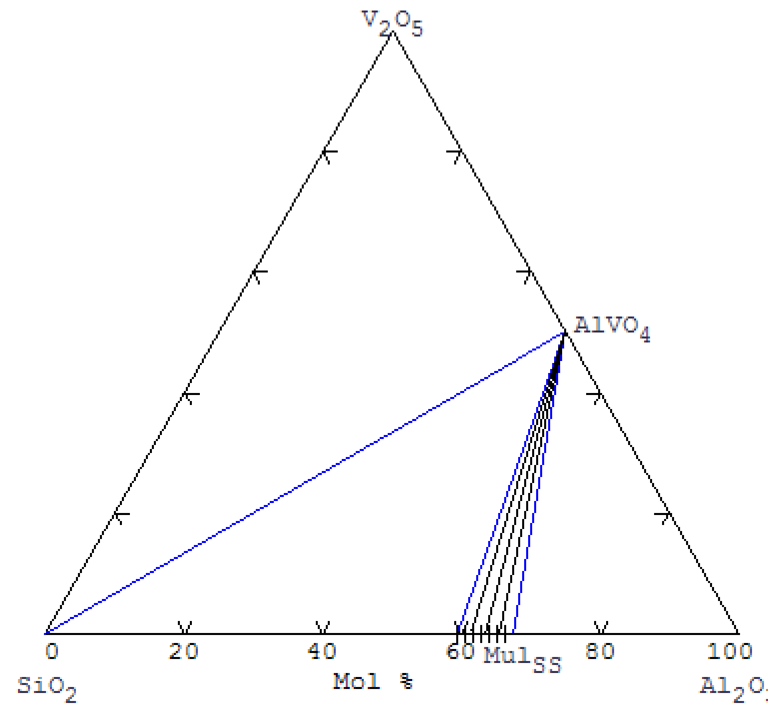

A.A. Fotiev, B.V. Slobodin, L.L. Surat, T.P. Sirina, Zh. Neorg. Khim., 28[4], (1983), pp. 588-591.

Isothermal section at 600°C in CaO-Fe_2O_3-V_2O_5

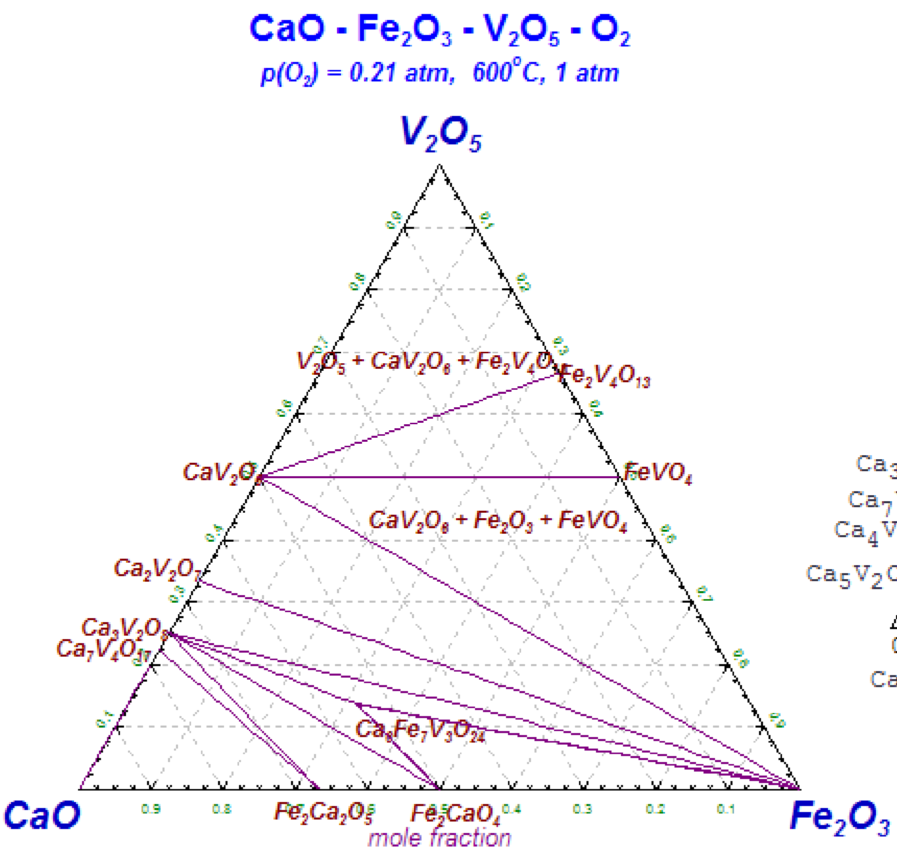

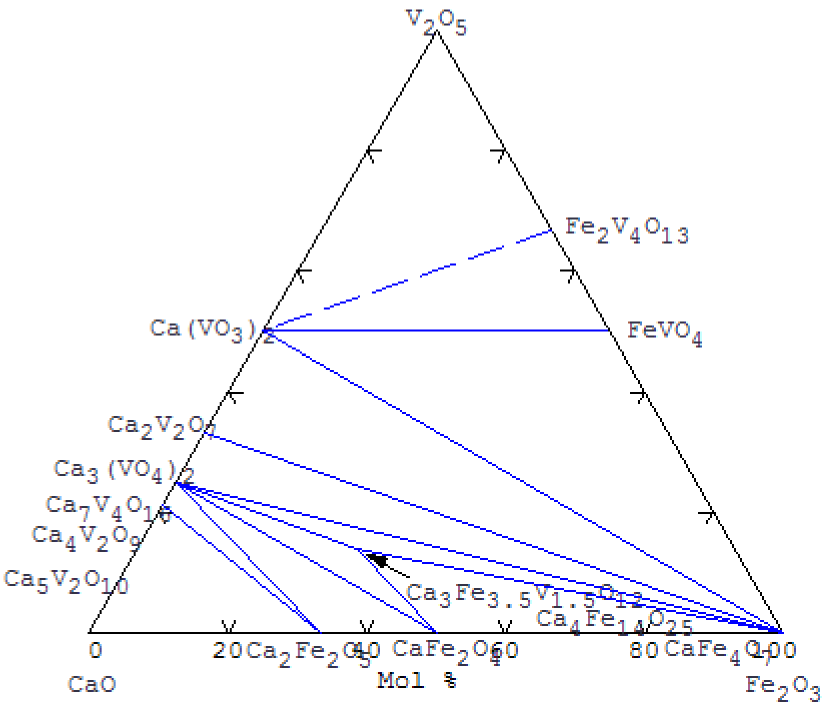

B.V. Slobodin, A.A. Fotiev, S.F. Blinova, Zh. Neorg. Khim., 24 [8], (1979), pp. 2276-2278.

Isothermal section at 600^oC in CaO-NiO-V_2O_5

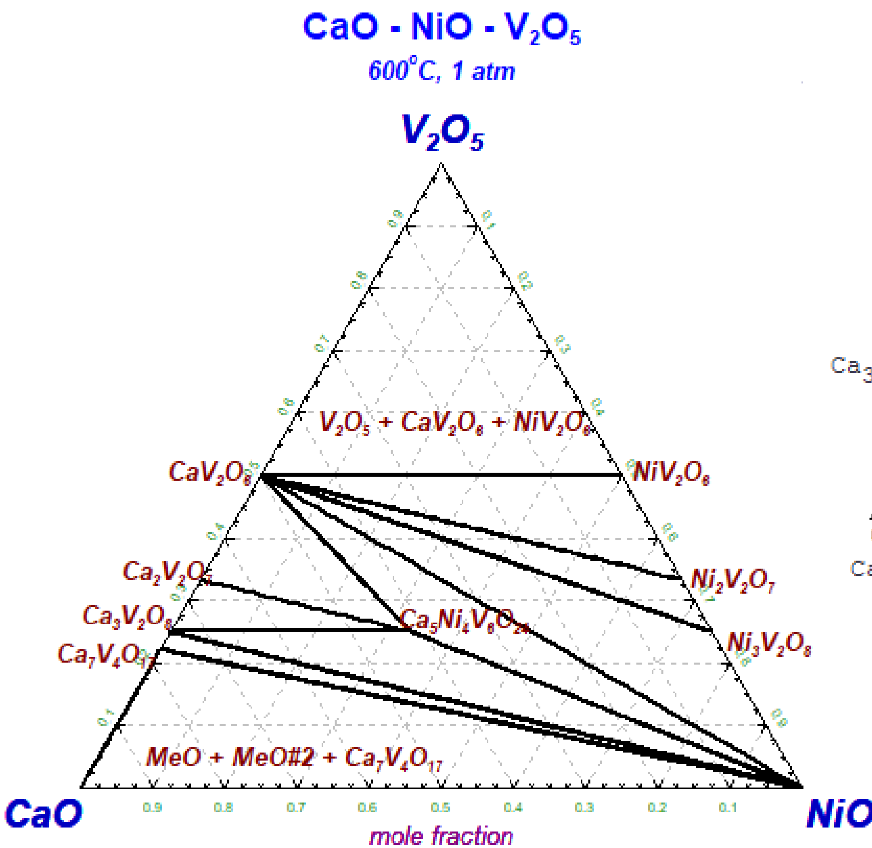

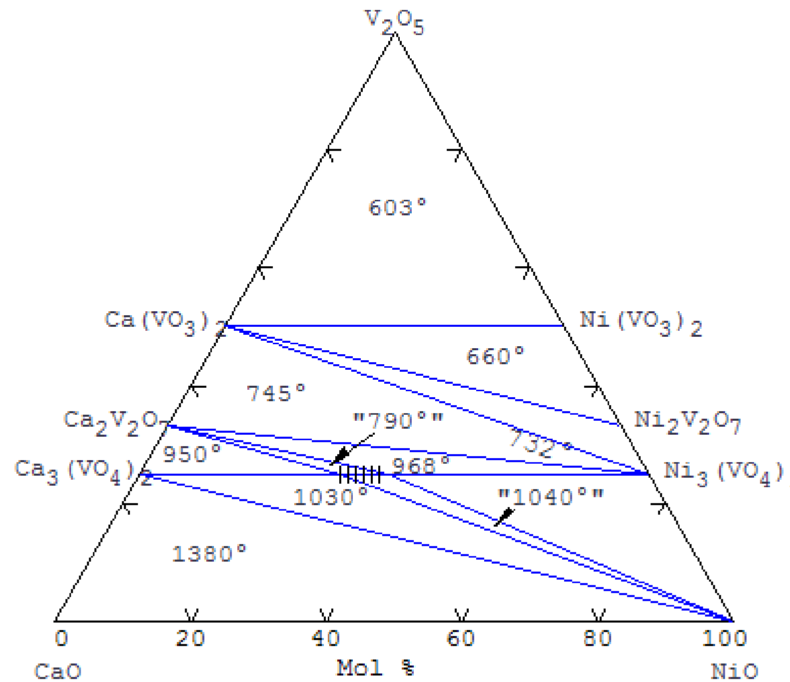

I.A. Arapova, N.P. Tugova, N.G. Sharova, B.V. Slobodin, Zh. Neorg. Khim., 26 [1], (1981), pp.281-282.

Isothermal section at 1500ºC in CaO-V_2O_5-SiO_2

GTT-Technologies

***C2S-C3P*– solid solution phase α-Ca_2SiO_4 with solubility for CrO,MgO,MnO and α'-$Ca_3P_2O_8$ with solubility for MgO. $(\underline{Ca^{+2}},Cr^{+2},Mg^{+2},Mn^{+2})_3(\underline{Ca^{+2}},\underline{Va})(\underline{P^{+5}},\underline{Si^{+4}},V^{+5})_2(O^{-2})_8$ with end-members:**

Ca_2SiO_4	$Ca_3P_2O_8$

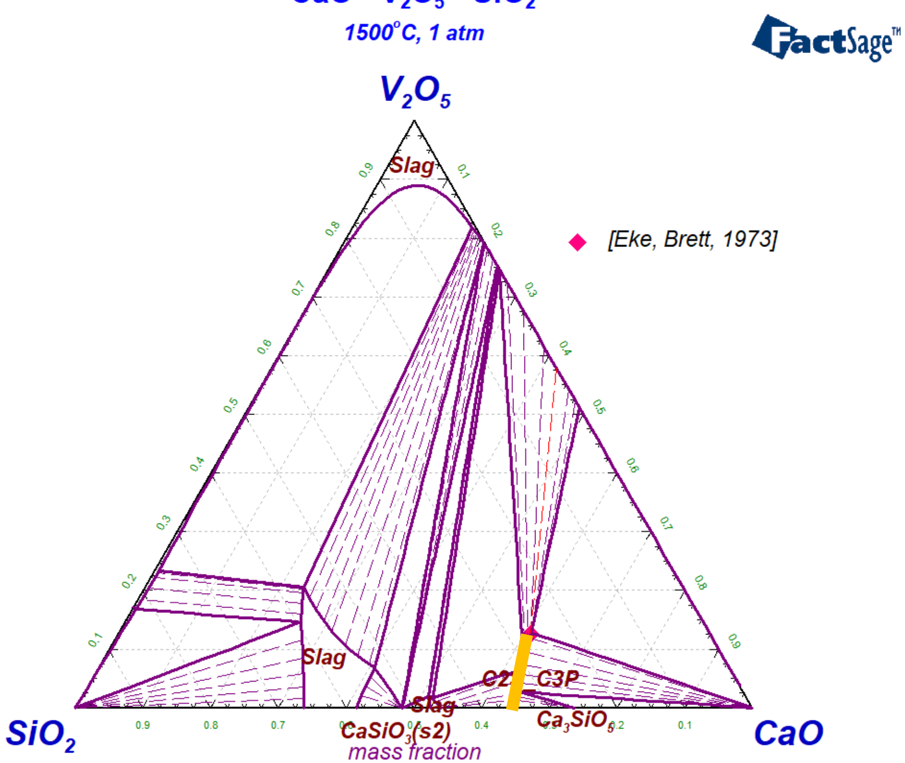

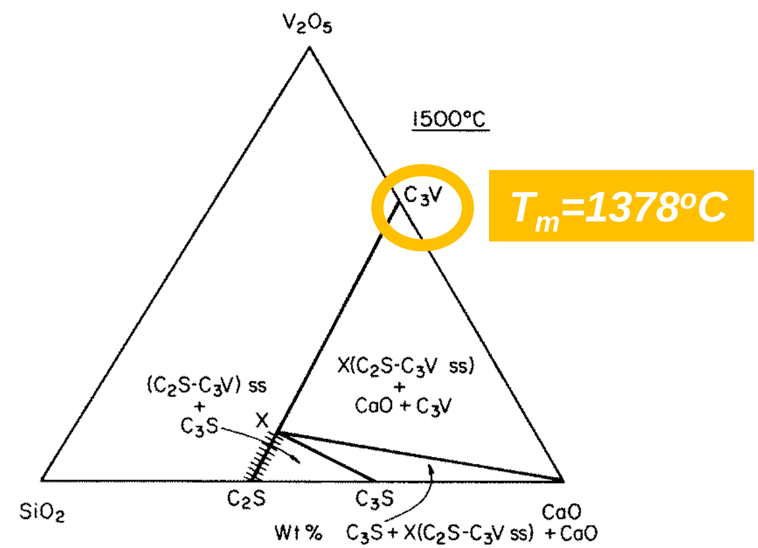

M. Eke, N.H. Brett, Trans. J. Br. Ceram. Soc., 72 [5], (1973), pp. 195-201.

Isothermal section at 1200°C in TiO_2-Ti_2O_3-V_2O_3

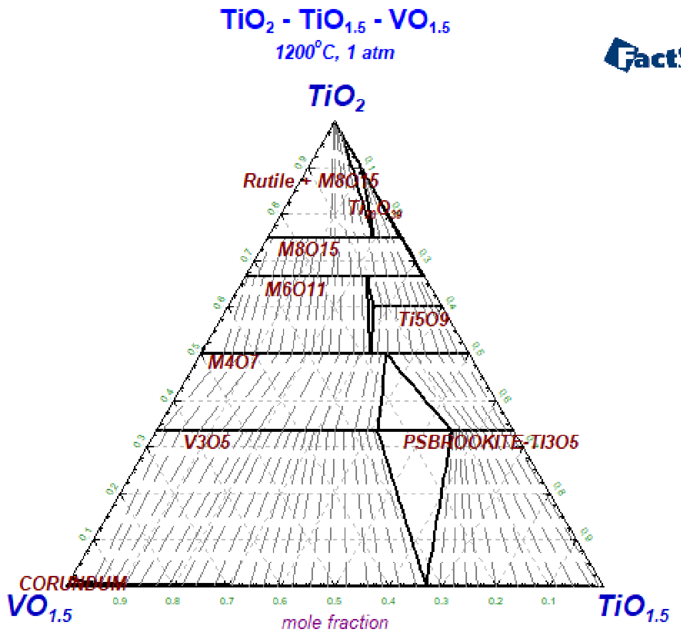

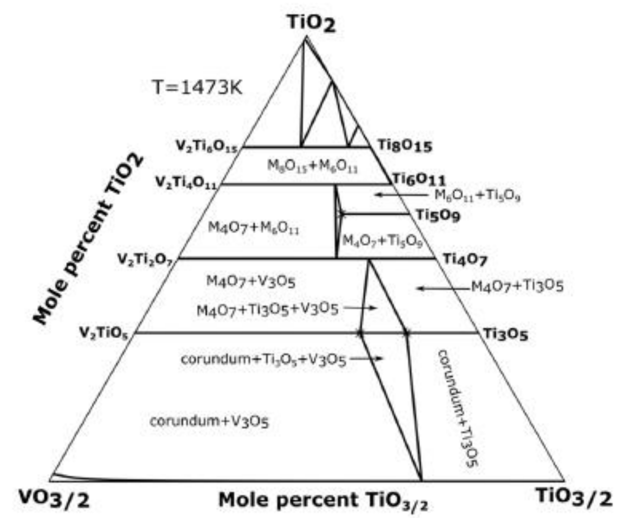

Fig. 5. Calculated isothermal section of the V_2O_3-Ti_2O_3-TiO_2 system at 1473 K. (The star symbols are the reported composition ranges for solid solutions, *viz*, $V_{0.69}Ti_{2.31}O_5$ for V_3O_5, $V_{0.42}Ti_{2.58}O_5$ for Ti_3O_5, $V_{0.665}Ti_{4.335}O_9$ for Ti_5O_9 [28].)

Phase	*Description*	*Used data*
Corundum	$(Ti^{+3},V^{+3},V^{+4})_2(Va)_1(O^{-2})_3$	Present work
Pseudobrookite	$(Ti, V)_1(Ti)_1(Ti)_1(O)_5$	Present work
Rutile	$(Ti, V)(O, Va)_2$	[Yang17]
V_3O_5	$(Ti, V)_3(O)_5$	[Yang17]
M_4O_7	$(Ti, V)_4(O)_7$	[Yang17]
V_5O_9	$(Ti, V)_5(O)_9$	[Yang17]
M_6O_{11}	$(Ti, V)_6(O)_{11}$	[Yang17]
M_8O_{15}	$(Ti, V)_8(O)_{15}$	[Yang17]

Conclusions

- The liquid phase in all subsystems was evaluated using associate species model (two cations per species).
- All available experimental information was used.
- 1 binaries, 14 quasi-binaries and 7 ternary systems were assessed.
- The solubility ranges of 20 Vanadium containing solid solution phases were modelled.

Thanks for your attention